Eur. Phys. J. B **56**, 199–203 (2007)
DOI: 10.1140/epjb/e2007-00118-3

THE EUROPEAN PHYSICAL JOURNAL B

Quantum phase transitions in the bosonic single-impurity Anderson model

H.-J. Lee and R. Bulla[a]

Theoretische Physik III, Elektronische Korrelationen und Magnetismus, Institut für Physik, Universität Augsburg, 86135 Augsburg, Germany

Received 15 September 2006 / Received in final form 29 March 2007
Published online 4 May 2007 –

Abstract. We consider a quantum impurity model in which a bosonic impurity level is coupled to a non-interacting bosonic bath, with the bosons at the impurity site subject to a local Coulomb repulsion U. Numerical renormalization group calculations for this bosonic single-impurity Anderson model reveal a zero-temperature phase diagram where Mott phases with reduced charge fluctuations are separated from a Bose-Einstein condensed phase by lines of quantum critical points. We discuss possible realizations of this model, such as atomic quantum dots in optical lattices. Furthermore, the bosonic single-impurity Anderson model appears as an effective impurity model in a dynamical mean-field theory of the Bose-Hubbard model.

PACS. 05.10.Cc Renormalization group methods – 05.30.Jp Boson systems – 03.75.Nt Other Bose-Einstein condensation phenomena

1 Introduction

The focus of this work is the physics of a bosonic impurity state coupled to a non-interacting bosonic environment modeled by the Hamiltonian

$$H = \varepsilon_0 b^\dagger b + \frac{1}{2} U b^\dagger b \left(b^\dagger b - 1\right) + \sum_k \varepsilon_k b_k^\dagger b_k + \sum_k V_k \left(b_k^\dagger b + b^\dagger b_k\right). \quad (1)$$

The energy of the impurity level (with operators $b^{(\dagger)}$) is given by ε_0; the parameter U is the local Coulomb repulsion acting on the bosons at the impurity site. The impurity couples to a bosonic bath via the hybridization V_k, with the bath degrees of freedom given by the operators $b_k^{(\dagger)}$ with energy ε_k.

We term the system defined by equation (1) the 'bosonic single-impurity Anderson model' (bosonic siAm), in analogy to the standard (fermionic) siAm [1] which has a very similar structure except that all fermionic operators are replaced by bosonic ones. Furthermore, we do not consider internal degrees of freedom of the bosons, such as the spin (an essential ingredient in the fermionic siAm).

There are various ways to motivate the study of the model equation (1). From a purely theoretical point of view it is interesting to compare the physics of the fermionic and bosonic versions of the siAm. Of course, there are striking differences between these two models: there is no direct bosonic analog of local moment formation and screening of these local moments at low temperatures, characteristics of the fermionic Kondo effect [2]. On the other hand, the bosonic model allows for a Bose-Einstein condensation (BEC), at least in a certain parameter space (see Fig. 1 below), a phenomenon which is clearly absent in the fermionic model.

There are certain similarities between the fermionic and the bosonic model concerning the role of the local Coulomb repulsion U: increasing the value of U can induce a quantum phase transition from a phase with screened spin to a local moment phase in the fermionic case [3], while it can induce a quantum phase transition from a BEC phase to a 'Mott phase' in the bosonic case, as shown below.

Another motivation for studying the bosonic siAm comes from a treatment of the Bose-Hubbard model within dynamical mean-field theory (DMFT) [4]. Although such an investigation has not been pursued so far, it is clear that the effective impurity model onto which the Bose-Hubbard model is mapped will have a similar form as equation (1) (see also Ref. [5]). An obvious application of such a DMFT treatment would then address the Mott transition in the Bose-Hubbard model [6] which must have its counterpart on the level of the effective impurity model — and the 'Mott transition' on the impurity level is precisely what we are looking at here.

Finally, a physical system described by the bosonic siAm could be directly realized in optical lattices ('atomic quantum dots', see Refs. [7,8]) or generally in optical

[a] e-mail: ralf.bulla@physik.uni-augsburg.de

traps. In the spirit of the 'Hubbard tool-box' [8,9], the laser fields in these systems could be tuned in such a way that a single impurity — a deep hole — is formed within an otherwise unperturbed system. Present theoretical studies of atomic quantum dots focus, however, on a coupling between impurity and excitations of the superfluid environment [7], for which a description in terms of the spin-boson model is more appropriate.

For the calculations presented in this paper we use the numerical renormalization group (NRG) originally developed by Wilson for the Kondo problem [10]. This method has been shown to give very accurate results for a broad range of impurity models, including the fermionic siAm [1,11] but also quantum impurities with coupling to a bosonic bath [12,13]. In Section 2 we briefly describe the bosonic extension of the NRG (bosonic NRG) which we employ here to study the model equation (1). Section 3 contains results for the ground state phase diagram of the bosonic siAm. We find that, similar to the Bose-Hubbard model, the phase diagram of the impurity model is characterized by a sequence of Mott phases, separated by lines of quantum critical points from a BEC phase. The paper is summarized in Section 4.

2 Model and method

Let us first discuss some general properties and trivial limits of the model equation (1). Similar to other quantum impurity models, the influence of the bath on the impurity is completely specified by the bath spectral function

$$\Delta(\omega) = \pi \sum_k V_k^2 \delta(\omega - \varepsilon_k). \tag{2}$$

Here we assume that $\Delta(\omega)$ can be parametrized by a powerlaw for frequencies up to a cutoff ω_c (we set $\omega_c = 1$ in the calculations)

$$\Delta(\omega) = 2\pi\,\alpha\,\omega_c^{1-s}\,\omega^s\,,\ 0 < \omega < \omega_c. \tag{3}$$

The parameter α is the dimensionless coupling constant for the impurity-bath interaction. This form of $\Delta(\omega)$ is certainly not the most general one and specific applications (within a bosonic DMFT or for an impurity level in an optical lattice) will lead to additional structures in $\Delta(\omega)$.

The NRG calculations presented here are performed for a grand-canonical ensemble with the chemical potential of the bath set to $\mu = 0$. Note that in the actual numerical calculation there is always a small gap between the chemical potential and the energy of the lowest bath state due to the discretization of the bath. Therefore a Bose-Einstein condensation of the whole system (impurity plus bath) can only be induced by the coupling to the impurity. This can already be seen in the non-interacting case, $U = 0$: here a direct diagonalization of the bosonic siAm shows that with increasing α, a localized state with *negative* energy separates out of the continuum at a critical value $\alpha = \alpha_c$. Right at the critical value, the BEC occurs via populating this localized state (the non-interacting model for $\alpha > \alpha_c$ is ill-defined as the ground-state has infinite negative energy, in contrast to the case of finite and positive U).

We want to stress here that, in general, a macroscopic occupation of such a localized state — which occupies a small area in real space around the impurity — cannot be realized for any finite repulsive interaction between the bosons in the bath [14]. The BEC phase of the bosonic siAm should therefore be regarded as an artefact of the model equation (1), for both $U = 0$ and finite U at the impurity site, although such a finite U prevents a macroscopic occupation of the impurity (see Fig. 4).

The other trivial limit of the bosonic siAm is the decoupled impurity, $\alpha = 0$. The succession of quantum phase transitions as shown in Figure 1 for $\alpha = 0$ can be easily understood from the dependence of the many-particle levels on the parameters ε_0 and U. The transition occurs for $\varepsilon_0/U = -n_{\rm imp}$ when the energies of the states with $n_{\rm imp}$ and $n_{\rm imp} + 1$ bosons are degenerate.

The full phase diagram Figure 1 is calculated with the bosonic NRG [13]. In this approach, the frequency range of the bath spectral function $[0, \omega_c]$ is divided into intervals $[\omega_c \Lambda^{-(n+1)}, \omega_c \Lambda^{-n}]$, $n = 0, 1, 2, \ldots$, with Λ the NRG discretization parameter (we use $\Lambda = 2.0$ for all the results shown in this paper). The continuous spectral function within these intervals is approximated by a single bosonic state and the resulting discretized model is then mapped onto a semi-infinite chain with the Hamiltonian

$$H = \varepsilon_0 b^\dagger b + \frac{1}{2} U b^\dagger b \left(b^\dagger b - 1\right) + V\left(b^\dagger \bar{b}_0 + \bar{b}_0^\dagger b\right) + \sum_{n=0}^{\infty} \varepsilon_n \bar{b}_n^\dagger \bar{b}_n + \sum_{n=0}^{\infty} t_n \left(\bar{b}_n^\dagger \bar{b}_{n+1} + \bar{b}_{n+1}^\dagger \bar{b}_n\right). \tag{4}$$

Here the impurity couples to the first site of the chain via the hybridization $V = \sqrt{2\alpha/(1+s)}$. The bath degrees of freedom are in the form of a tight-binding chain with operators $\bar{b}_n^{(\dagger)}$, on-site energies ε_n, and hopping matrix elements t_n which both fall off exponentially: $t_n, \varepsilon_n \propto \Lambda^{-n}$.

The chain model equation (4) is diagonalized iteratively starting with the impurity site and adding one site of the chain in each iteration. As for the application to the spin-boson model, only a finite number N_b of basis states for the added site can be taken into account, and, after diagonalizing the enlarged cluster, only the lowest-lying N_s many-particle states are kept for the subsequent iterations (here we use $N_b = 10$–20 and $N_s = 100$–200). The main technical difference to the spin-boson model is that we can use the total particle-number as a conserved quantity in the Hamiltonian equation (1). Furthermore, the renormalization group flow turns out to be considerably more stable as in the calculations for the spin-boson model so that we can easily perform up to $N = 100$ iterations.

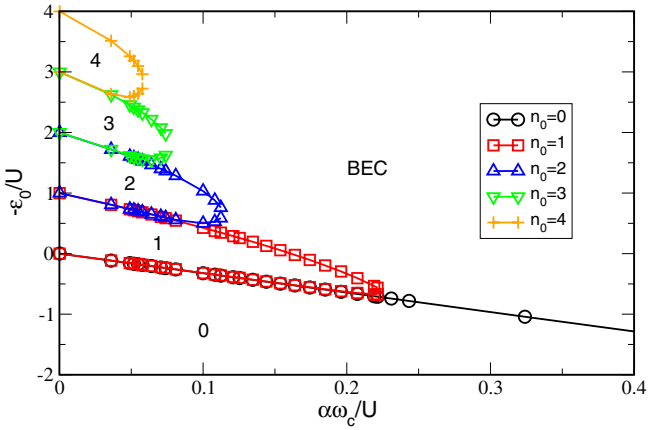

Fig. 1. Zero-temperature phase diagram of the bosonic siAm for bath exponent $s = 0.6$ and fixed impurity Coulomb interaction $U = 0.5$. The different symbols denote the phase boundaries between the Mott phases and the BEC phase. The Mott phases are labeled by their occupation $n_0 = n_{\rm imp}$ ($\alpha = 0$). Only the Mott phases with $n_0 \leq 4$ are shown. The NRG parameters are $\Lambda = 2.0$, $N_{\rm b} = 10$, and $N_{\rm s} = 100$.

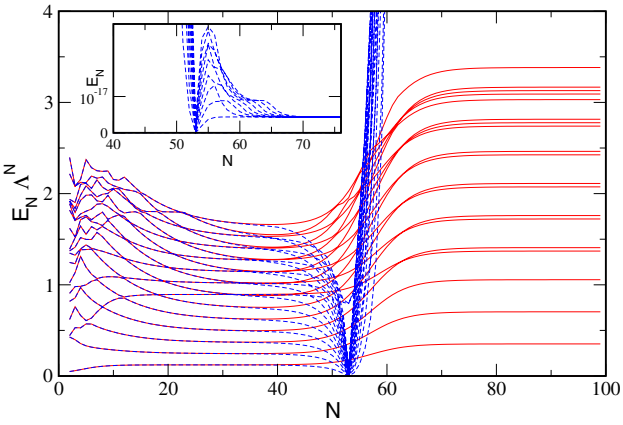

Fig. 2. Flow diagram of the lowest lying many-particle levels E_N versus iteration number N for parameters $s = 0.4$, $\alpha = 0.007$, $U = 0.5$, and two values of ε_0 very close to the quantum phase transition between the Mott phase with $n_0 = 2$ and the BEC phase. Both the quantum critical point and the Mott phase appear as fixed points in this scheme whereas in the BEC phase, a gap $\Delta_{\rm g}$ opens between the ground state and the first excited state, see the inset where E_N (instead of $E_N \Lambda^N$) is plotted versus N.

3 Results

Let us now discuss the $T = 0$ phase diagram of the bosonic siAm, Figure 1, calculated for fixed $U = 0.5$ with the parameter space spanned by the dimensionless coupling constant α and the impurity energy ε_0. We choose $s = 0.6$ as the exponent of the powerlaw in $\Delta(\omega)$ (the s-dependence of the phase diagram is discussed in Fig. 5 below). The phase diagram is characterized by a sequence of lobes which we label by the impurity occupation $n_0 = n_{\rm imp}(\alpha = 0)$ where it takes integer values. We use the terminology 'Mott phases' for these lobes, due to the apparent similarity to the phase diagram of the Bose-Hubbard model. The Mott phases are separated from the BEC phase by lines of quantum critical points which terminate (for $s = 0.6$) at a finite value of α, except for the $n_0 = 0$ phase where the boundary extends up to infinite α. These transitions can be viewed as the impurity analogue of the Mott transition in the lattice model, since it is the local Coulomb repulsion which prevents the formation of the BEC state.

The phase diagram Figure 1 is deduced from the flow of the lowest-lying many-particle levels which allows quite generally to identify fixed points and transitions between these fixed points [11]. Figure 2 shows the flow for $s = 0.4$, fixed $\alpha = 0.007$ and $U = 0.5$, and two values of ε_0 very close to the quantum phase transition. The solid lines belong to the Mott phase with $n_0 = 2$ and display a crossover between two fixed points: from an unstable quantum critical point for iteration numbers $N \sim 20$–40 to a stable fixed point for $N > 70$. Analysis of the stable fixed point shows that it can be described by a decoupled impurity with occupation $n_0 = 2$ and a free bosonic bath given by the decoupled chain. (The actual impurity occupation $n_{\rm imp}$, however, differs from the integer values, as discussed below.) The structure of the quantum critical point, on the other hand, is presently not clear but might be accessible to perturbative methods as discussed in [15].

The dashed lines belong to the BEC phase where, apparently, something dramatic is happening at $N \approx 55$. The divergence of the energies for all excited states seen in this plot is due to the formation of a localized state, split off from the continuum by an energy gap $\Delta_{\rm g}$. This energy gap, which can be viewed as the order parameter of the BEC phase, takes a finite value which is not renormalized to zero as Λ^{-N} as the levels of the other fixed points, therefore the divergence of $\Delta_{\rm g} \cdot \Lambda^N$. In the inset of Figure 2 we plot E_N (instead of $E_N \Lambda^N$) so that the development of the gap $\Delta_{\rm g} \approx 4 \times 10^{-18}$ appears as a plateau of the first excited state. The extremely small value of the gap is due to the tuning of the parameters very close to the transition; it turns out that $\Delta_{\rm g}$ vanishes at the transition with a powerlaw, with the same exponent as the crossover scale T^*, as discussed below. Further analysis of the data shows that the ground state in the BEC phase has an occupation number given by the maximum boson number used in the iterative diagonalization.

The fact that the unstable fixed point separating the Mott phase from the BEC phase is indeed a quantum critical point can be deduced from its non-trivial level structure, as mentioned above, and the behavior of the crossover scale T^*. Numerically we find that upon variation of ε_0 close to its critical value $\varepsilon_{0,\rm c}$, the crossover scale vanishes with a powerlaw at the transition, $T^* \propto |\varepsilon_0 - \varepsilon_{0,\rm c}|^\nu$. (Upon variation of α, the relation is $T^* \propto |\alpha - \alpha_{\rm c}|^\nu$.) This can be seen in the inset of Figure 3, where we also show that the same critical exponent obtains upon variation of α below and above the critical value. For $s = 0.4$, we find an exponent $\nu \approx 2.50 \pm 0.06$, valid for all lines of quantum critical points in the phase diagram for this value of the bath exponent.

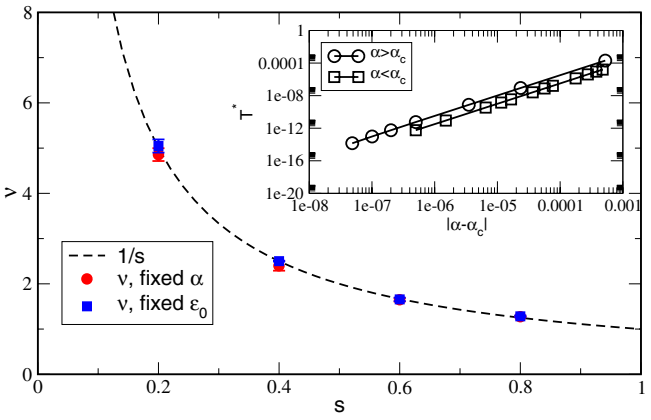

Fig. 3. Main panel: dependence of the critical exponent ν on the bath exponent s, calculated upon variation of ε_0 (circles) and α (squares). Data are in very good agreement with the relation $\nu = 1/s$, plotted as dashed line. The inset shows the dependence of the crossover scale T^* on $|\alpha - \alpha_c|$ for fixed $\varepsilon_0 = -0.25$, $U = 0.5$, $s = 0.4$, and for α-values on both sides of the transition (squares: $\alpha < \alpha_c$, circles: $\alpha > \alpha_c$).

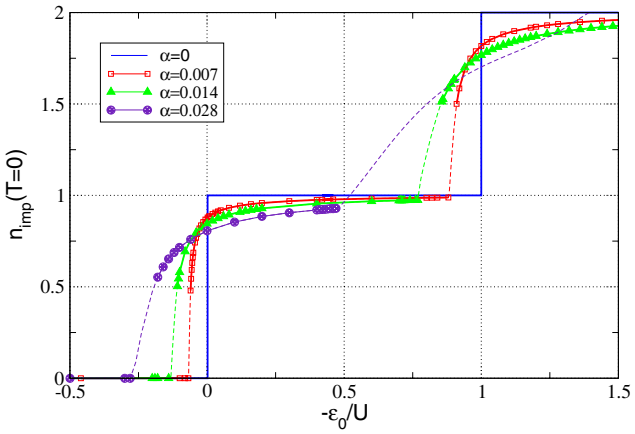

Fig. 4. Impurity occupation $n_{\rm imp}$ as a function of ε_0 for temperature $T = 0$, $s = 0.4$, $U = 0.5$, and various values of α. The sharp steps for the decoupled impurity $\alpha = 0$ are rounded for any finite α. Symbols (dashed lines) correspond to data points within the Mott (BEC) phases.

The dependence of the critical exponent ν on s is shown in the main panel of Figure 3. Our data suggest that the relation $\nu = 1/s$ is valid for the whole range, $0 < s < 1$. This relation also holds for the critical exponent corresponding to the vanishing of the order parameter, $\Delta_{\rm g}$, when approaching the transition from the BEC side.

Let us now focus on the impurity occupation $n_{\rm imp}$ for temperature $T = 0$. Figure 4 shows the dependence of $n_{\rm imp}$ on ε_0 for $s = 0.4$, $U = 0.5$, and various values of α. The symbols indicate that the system is in the Mott phase whereas the dashed lines are for the BEC phase. Taken together, both sets of lines form a continuous curve.

The terminology we use here suggests an integer occupation throughout the Mott phase, as for the Bose-Hubbard model, but for the bosonic siAm $n_{\rm imp}$ deviates from the integer values as soon as the coupling to the bath is finite, see Figure 4. This is to be expected since for a gapless bath spectral function $\Delta(\omega)$, the charge fluctuations on the impurity site cannot be completely suppressed. Indeed we observe that for increasing the value of the bath exponent s, the $n_{\rm imp}(\varepsilon_0)$-curve gets closer to the step function. At this point one can speculate about the possible development of $\Delta(\omega)$ in a DMFT treatment of the Mott phase. The self-consistency might generate a bath spectral function with a gap and the impurity occupation might then turn into the step function expected for the lattice model.

The precise shape of the boundaries in the phase diagram Figure 1 depends on the form of $\Delta(\omega)$ for *all* frequencies. Here we stick to the powerlaw form equation (3) and present the dependence of the phase diagram on the bath exponent s in Figure 5. We observe that upon increasing the value of s, the areas occupied by the Mott phases extend to larger values of α and significantly change their shape. A qualitative change is observed when the exponent approaches $s = 1$. First of all, the Mott phases appear to

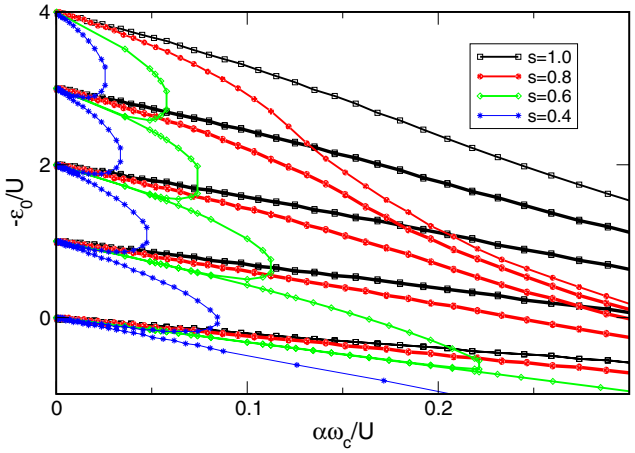

Fig. 5. Zero-temperature phase diagram of the bosonic siAm as in Figure 1, but now for different values of the bath exponent s. For increasing value of s, the areas occupied by the Mott phases significantly change their shape and for $s = 1$ it appears that each Mott phase extends up to arbitrarily large values of α.

extend up to arbitrarily large values of α. Furthermore, the BEC phase which separates the Mott phases for $s < 1$ and $\alpha > 0$ is completely absent for $s = 1$! We do not yet have an explanation for this observation and it would be interesting to find out whether the absence of the BEC phase is due to the special form of $\Delta(\omega)$, equation (3), or whether it is a generic feature even when $\Delta(\omega) \propto \omega$ is only valid for $\omega \to 0$.

In contrast, the Mott phase vanishes in the limit $s \to 0$: an extrapolation of the phase boundaries for values of s in the range $0.01 < s < 0.1$ clearly shows a powerlaw dependence: $\alpha_{\rm c}(s) \propto s^{\beta}$, with $\beta \approx 0.485 \pm 0.015$.

4 Summary

To summarize, we have presented NRG calculations for the phase diagram and the impurity occupation of a bosonic version of the single-impurity Anderson model. The phase diagram contains Mott phases, in which the local Coulomb repulsion prevents Bose-Einstein condensation, separated by the BEC phase by lines of quantum critical points. The BEC phase corresponds to a macroscopic occupation of a localized state around the impurity and it would be very interesting to study how this (artificial) property of the model changes when interactions between the bosons in the bath are taken into account, for example within a mean-field calculation.

In future, we are planning to calculate, for example, physical properties at finite temperatures and dynamic quantities (impurity spectral function and self-energy). The latter will be of importance for a possible DMFT for the Bose-Hubbard model, an approach which has not yet been fully developed. One important issue in this context is the proper scaling of the Hamiltonian parameters in the limit of infinite spatial dimensions [16]. For example, the model on a hypercubic lattice as studied in reference [17] requires a scaling of the hopping matrix elements as $1/d$ which leads to a static mean-field theory. Another issue is that the bosonic DMFT in the superfluid phase of the Bose-Hubbard model might generate a more complex impurity model, the bosonic siAm introduced here would then be applicable only within the Mott phases of the lattice model.

Finally, it would be interesting to identify situations for atomic quantum dots in optical lattices which can be described by the bosonic single-impurity Anderson model or generalizations thereof.

We would like to thank Krzysztof Byczuk, Jim Freericks, David Logan, Michael Potthoff, Matthias Vojta, and Dieter Vollhardt for helpful discussions. This research was supported by the DFG through SFB 484.

References

1. A.C. Hewson, *The Kondo Problem to Heavy Fermions* (Cambridge Univ. Press, Cambridge, 1993)
2. A bosonic analogue of the Kondo effect can be observed in the models proposed in S. Florens, L. Fritz, M. Vojta, Phys. Rev. Lett. **96**, 036601 (2006); these models are not directly related to the bosonic siAm studied here
3. Such a quantum phase transition is seen, for example, in the soft-gap Anderson and Kondo models, see M. Vojta, Phil. Mag. **86**, 1807 (2006), and references therein
4. For the DMFT for fermionic models, see W. Metzner, D. Vollhardt, Phys. Rev. Lett. **62**, 324 (1989); A. Georges, G. Kotliar, W. Krauth, M.J. Rozenberg, Rev. Mod. Phys. **68**, 13 (1996)
5. R. Bulla, Phil. Mag. **86**, 1877 (2006)
6. M.P.A. Fisher, P.B. Weichman, G. Grinstein, D.S. Fisher, Phys. Rev. B **40**, 546 (1989)
7. A. Recati, P.O. Fedichev, W. Zwerger, J. von Delft, P. Zoller, Phys. Rev. Lett. **94**, 040404 (2005)
8. D. Jaksch, P. Zoller, Ann. Phys. **315**, 52 (2005)
9. M. Lewenstein, A. Sanpera, V. Ahufinger, B. Damski, A. Sen De, U. Sen, e-print `arXiv:cond-mat/0606771` (2006)
10. K.G. Wilson, Rev. Mod. Phys. **47**, 773 (1975)
11. R. Bulla, T. Costi, Th. Pruschke, e-print `arXiv: cond-mat/0701105` (2007)
12. R. Bulla, N.-H. Tong, M. Vojta, Phys. Rev. Lett. **91**, 170601 (2003)
13. R. Bulla, H.-J. Lee, N.-H. Tong, M. Vojta, Phys. Rev. B **71**, 045122 (2005)
14. Bose-Einstein condensation in the presence of an attractive δ-function impurity has been studied for non-interacting bosons in: S. Goulart Rosa, Jr, O. Hipólito, R. Lobo, Phys. Rev. A **11**, 1454 (1975)
15. H.-J. Lee, R. Bulla, M. Vojta, J. Phys.: Condens. Matter **17**, 6935 (2005)
16. D. Vollhardt, private communication
17. J.K. Freericks, H. Monien, Phys. Rev. B **53**, 2691 (1996)